RSC Advances

ROYAL SOCIETY OF CHEMISTRY

www.rsc.org/advances

The evaluation of cellular uptake efficiency and tumor-target ability of MPEG-PDLLA micelles: Effect of particle size

Ying Hao[1], YiXing Huang[2, +], YunQi He[3], JinRong Peng[1], LiJuan Chen[1], Xun Hu [4, *], ZhiYong Qian[1,*]

[1]State Key Laboratory of Biotherapy and Cancer Center, West China Hospital, Sichuan University, and Collaborative Innovation Center for Biotherapy, Chengdu, 610041, PR China

[2]Department of Orthopaedic Surgery, Second Affiliated Hospital of Wenzhou Medical University, Wenzhou Medical University, 109 Xueyuan Road, Wenzhou, 325027, China.

[3]College of Chemistry, Sichuan University, Chengdu, 610064, PR China

[4] Biobank of West China Hospital, Sichuan University, Chengdu, 610041, PR China

Abstract

In this study, we successfully prepared the MPEG-PDLLA polymer micelles with two different particle sizes A and B. DLS and TEM assays demonstrated that the particle size of the polymer micelles A and the polymer micelles B were about 25 nm and 150 nm respectively. The stability of the MPEG-PDLLA polymer micelles *in vitro* revealed that the free cy5.5 dye had been successfully loaded into the polymer micelles as a fluorescence marker and the fluorescence wasn't quenched until 72 h. The cellular uptake of the polymer micelles was time-dependent and the micelles A (particle size 25 nm) showed a higher efficiency to be internalized into the cytoplasm of MCF-7 cells than the micelles B (particle size 150 nm). Furthermore, *in vivo* and *in vitro* biodistribution and tumor-target of polymer micelles MPEG-PDLLA were

+ Huang YX is the co-first author with Hao Y.

*Hu X and Qian ZY are the co-corresponding authors for this work, Tel/Fax: +86-28-85501986,E-mail: anderson-qian@163.com (Qian ZY), and Tel/Fax: +86-28-85164085, E-mail: hxxhu99@163.com (Hu X).

investigated in female MCF-7 tumor-bearing balb/cA-nu mice with an IVIS imaging system. The results showed that the polymer micelles A (particle size 25 nm) had a time dependent biodistribution and tumor sites accumulation in mice bearing MCF-7 tumors. Meanwhile, the NIR fluorescence intensity of the polymer micelles B (particle size 150 nm) in tumor sites showed a pattern of a rise, a peak and then a decline. What's more, the distribution of the polymer micelles in the tissue slices demonstrated the same results. Consequently, the results indicated that the micelles with smaller particle size (25 nm) could be more efficiently internalized into cells and enhance permeation and retention (EPR) effect in tumor tissue. Therefore, a reasonable small size of micelles may be a key factor for a high-performance anti-cancer drug delivery system.

Keywords

MPEG-PDLLA polymer micelles, particle size, cellular uptake, biodistribution, tumor-target, enhance permeation and retention (EPR) effect.

Introduction

Nowadays, more and more people are suffering from cancer, but the traditional anti-cancer drugs have a lot of drawbacks, such as being poorly water-soluble [1,2], having side effects and multidrug resistance [3,4]. Nanotechnology high lights the hope for cancer therapy as a large number of nano carriers are used in clinical. [5-8].

In recent years, amphiphilic block copolymers have attracted significant attention as a means of delivering anti-cancer drugs because amphiphilic block copolymers consist of hydrophilic and hydrophobic segments, which have the ability to form nano carriers and self-assemble in aqueous solutions [9-11]. Nano carriers can not only transport anticancer agents, but also have same advantages such as long-circulating time, high cellular uptake efficiency and preferentially reach tumor sites [12,13]. What's more, they have shown different cellular uptake efficiency and tumor targeting abilities depending on their sizes [14-16]. There have been proved that the particle sizes ranging from 25 to 50 nm are suitable for achieving high cellular uptake efficiency as the cellular uptake of nano carriers are regulated by membrane tension,

the optimal radius for endocytosis is on the order of 25-50 nm [17-20]. Additionally, nano carriers in the size range of 10-200 nm are highly recommended for tumor accumulation, owing to the advantages of reducing clearance from the reticuloendothelial system (RES), and increasing tumor accumulation through enhance permeation and retention (EPR) effect [8,21].

Among amphiphilic block copolymers [22-24], monomethoxy poly (ethylene glycol)-poly (D, L-lactic acid) copolymer (MPEG-PDLLA) has sparked interest as drug delivery carriers [25]. MPEG-PDLLA consists of polyethylene glycol (MPEG) and poly (D,L-lactide), which are FDA-approved non-cytotoxic, non-immunogenic polymer and has been widely used as a long-circulating agent to improve biocompatibility, stability and have a good record of offering great potential for controlled release [26,27]. Samyang's proprietary polymeric micelle technology utilizing PTX loaded MPEG-PDLLA (Mn = 3765) micelles (Genexol-PM®) for cancer chemotherapeutic was applied in the clinic and approved in Korea in 2006 [28]. In additional, the study on MPEG-PDLLA is carrying on [29-32]. However, the study on particle size of the nano carrier MPEG-PDLLA is still needed to develop as the particle size determines the mechanism and rate of cell uptake of nano carriers and its ability to permeate through tissue [33]. The particle size less than 5 nm is rapidly cleared from the circulation through renal clearance or extravasation, and as particle size increases to 15 μm, the accumulation occurs primarily in the liver, the spleen and the bone marrow which may cause certain toxicity [34, 35]. It is necessary to study the influence of particle size of nano carrier MPEG-PDLLA immediately and make sure which size of MPEG-PDLLA is a promising nano carrier.

In this study, we aimed to evaluate the cellular uptake efficiency and tumor-target ability of MPEG-PDLLA micelles with two different particle sizes 25 nm and 150 nm. As the MPEG-PDLLA had no fluorescent group, we chose Cy5.5-NHS ester as a fluorescent marker [36-39]. Cy5.5-NHS ester was a fluorescent marker in the near infrared region (NIR) spectrum, which was suitable for small animal *in vivo* live imaging instead of radioactive elements imaging [40-42]. We used two methods to get MPEG-PDLLA micelles with two different particle sizes. The cellular uptake

efficiency of the micelles was investigated in MCF-7 cells. Then we detected the biodistribution and tumor-target of the MPEG-PDLLA micelles with different particle sizes by an IVIS imaging system. This study is the first time an IVIS imaging system has been used to detect the biodistribution and tumor-target of MPEG-PDLLA with two different particle sizes, which was more sensitive, cost-effective, easy-of-use, and avoiding the use of radiopharmaceuticals. We could easily get the real-time difference of biodistribution between MPEG-PDLLA with different particle sizes through the IVIS imaging system, and the results could be intuitive to see whether the same nano carrier with different particle sizes have different delivery efficiency, and which particle size of MPEG-PDLLA micelles is suitable for delivering anti-cancer drug.

Materials and Experimental Methods

Materials

Monomethoxy-poly (ethylene glycol) with a molecular weight of 2000 (MPEG 200 0), Stannous Octoate ($Sn(Oct)_2$), Dicyclohexylcarbodiimide (DCC) and N-(tert-buto xycarbonyl)-L-alanine (BOC-L-AlA) were obtained from Sigma Aldrich Company. D, L-lactide was purchased from Beijing Jiankai Corporation in China. Anhydrous ethanol was purchased from Shanghai Aladdin company. Cy5.5-NHS ester was purchased from Beijing Fanbobiochemicals company. All the materials used in this article were analytic grade and used as received.

An MCF-7 cell line was obtained from the American Type Culture Collection (ATCC; Rockville, MD) and grown in RPMI DMEM media with 10 % FBS and 1 % antibiotics. The cell culture was maintained in a 37 ^{o}C incubator with a humidified 5 % CO_2 atmosphere.

Balb/cA-nu mice used for *in vivo* and *in vitro* fluorescence imaging were purchased from the HFK Bio-Technology. Co., LTD (Beijing, China). Throughout the experiment, the animals were housed at a temperature of 20 ± 2 ^{o}C, relative humidity of 50-60 %, and with 12 h light-dark cycles. All animal care and experimental procedures were conducted according to Institutional Animal Care and Use guidelines.

Synthesis of MPEG-PDLLA-NH_2

MPEG-PDLLA copolymer (2000-1765) was synthesized by ring opening polymerization. 17.65 g D, L-lactide and 20 g MPEG 2000 were put into a dried glass reactor already flame-dried and purged three times by nitrogen. Then 0.3 % stannous octoate (0.113 g) was added in an environment of nitrogen. The polymerization started in the oil bath at 150 ^{o}C for 9 h. After the completion of the reaction, the products were dissolved in 50 mL ethanol, then precipitated in 500 mL cold n-pentane and filtered three times. The final copolymer was kept in a vacuum at 35 ^{o}C for 48 h [43].

The diblock copolymer MPEG-PDLLA was converted into BOC-L-AlA as follows: a nitrogen-purged flask containing 10.0 g MPEG-PDLLA and 4.0 g BOC-L-AlA dissolved in 100 mL anhydrous CH_2Cl_2 was treated with a solution of 3.0 g DCC for 72 h at 25 ^{o}C. The dicyclohexylurea was removed by vacuum filtration. The filtrate was washed with 100 mL saturated aqueous $NaHCO_3$ and 100 mL distilled water three times. Then the copolymer was obtained by removing the organic solvents in a vacuum by a rotary evaporator [44].

MPEG-PDLLA-NH_2 was synthesized by removing the tert-butoxycarbonyl end group from MPEG-PDLLA-BOC [45] as follows: 5 g MPEG-PDLLA-BOC was dissolved in 50 mL CH_2Cl_2. The solution was cooled to 0 ^{o}C and treated with 15 mL trifluoroaceticacid (TFA) for 2.5 h in an atmosphere of nitrogen. TFA was then removed in a vacuum, the residue was dissolved in 40 mL chloroform and washed with 100 mL saturated aqueous $NaHCO_3$ and 100 mL distilled water three times. Finally the copolymer was obtained by removing the organic solvents in a vacuum by a rotary evaporator.

Characterization of MPEG-PDLLA-NH_2

The diblock copolymer was characterized by ^{1}H NMR spectra (Varian 400 spectrometer, Varian, USA), FTIR (NICOLET 200SXV, Nicolet, USA) and GPC (Agilent 110 HPLC, USA) [46].

Synthesis of fluorescence marker MPEG-PDLLA-Cy5.5

MPEG-PDLLA-Cy5.5 was synthesized by reacting the Cy5.5-NHS ester (0.5 mg)

with MPEG-PDLLA-NH_2 (100 mg) dissolved in 5 mL dimethylsulfoxide at room temperature for 24 h [47, 48]. Then using a dialysis bag which molecular mass cutoff is 2 kDa to remove free Cy5.5-NHS and dimethylsulfoxide for 48 h. The final product was free-dried and stored at - 20 ^{o}C in the dark until used.

Preparation of the MPEG-PDLLA micelles

In this research, we used two methods to prepare MPEG-PDLLA micelles. One was a thin-film hydration method [29, 49]. Briefly, 30 mg MPEG-PDLLA and 1 mg MPEG-PDLLA-Cy5.5 were dissolved together in 4 mL anhydrous ethanol to prepare a polymer solution. Then a rotary evaporator was used to remove anhydrous ethanol in vacuum at 37 ^{o}C for 2 h. Finally, 4 mL distilled water were added to prepare micelles at 60 ^{o}C and filtered with a syringe filter (pore size: 220 nm) (Millex-LG, Millipore Co., USA). All operations were conducted in the dark.

The other method was an ethanol injection method [50, 51]. 30 mg MPEG-PDLLA and 1 mg MPEG-PDLLA-Cy5.5 were dissolved together in 4 mL ethanol. The mixed polymer in anhydrous ethanol was slowly added to 4 mL distilled water and stirred at 60 ^{o}C to remove anhydrous ethanol for about 5 h. Then micelles were filtered with a syringe filter (pore size: 220 nm) (Millex-LG, Millipore Co., USA). All operations were conducted in the dark.

The concentration of free dye group (control group) was 1.25 μg/mL that was same with the concentration of polymer micelles. The free Cy5.5 dye was hydrophobia, so we used 1 mL DMSO to dissolve 1 mg Cy5.5 dye to get 1 mg/mL stock solution. Then we took 1.25 μL stock solution (1 mg/mL) to dilute with saline to 1mL to get the free dye.

Characterization of the MPEG-PDLLA micelles

The particle size of the MPEG-PDLLA polymer micelles was measured by dynamic light scattering (DLS) (Nano-ZS90, Malvern, UK). The morphology of the polymer micelles was observed by a transmission electron microscope (TEM) (H-6009IV, Hitachi, Japan). Before using the TEM to observe, samples were placed on a carbon-coated copper grid, and negatively stained by phosphotungstic acids [52].

The stability of the MPEG-PDLLA micelles with Cy5.5 fluorescence marker

The stability of the MPEG-PDLLA polymer micelles was measured by a fluorescence spectrophotometer (Perkin Elmer, USA) [53]. We used fluorescence spectrophotometer to observe the fluorescence intensity at 5 min, 30 min, 1 h, 2 h, 4 h, 6 h, 8 h, 12 h, 24 h, 48 h and 72 h after the polymer micelles were prepared.

Cellular imaging

We used MCF-7 breast cancer cells to investigate the uptake of the MPEG-PDLLA polymer micelles [54-55]. First, MCF-7 breast cancer cells were seeded in 6-well plates (2×10^5) and incubated for 24 h. Then RPMI DMEM media were used with 2 mL 1.25 μg/mL polymer micelles and 1 % antibiotics (the RPMI DMEM media with 2 mL 1 % antibiotics was used as control group) to replace the RPMI DMEM media with 10 % FBS and 1 % antibiotics per well. Next they were incubated for an additional 30 min (1 h, 2 h, 4 h, 6 h). After removing the supernatant, the cells were fixed with 70 % ETOH for 15 min and then DAPI was added for a 10 min incubation. Subsequently, the cells were washed 3 times with PBS and sealed with glycerine. The cellular uptake of the polymer micelles was determined using a confocal laser scanning microscope (CLSM) from Germany Leica Corporation. The quantitative data was analyzed by flow cytometry from USA BD Bioscience Corporation.

***In vivo* and *in vitro* fluorescence imaging**

An *in vivo* and *in vitro* fluorescence imaging study was performed in female MCF-7 tumor-bearing balb/cA-nu mice [56, 57]. Tumors were initially established by injecting a mixture of 1×10^6 MCF-7 cells subcutaneously. When the tumors reached a volume of 200 mm^3, the biodistribution of the MPEG-PDLLA polymer micelles was studied by injecting 100 μL 1.25 μg/mL micelles (free cy5.5) intravenously through a tail vein of mice bearing MCF-7 tumors. These were imaged at 5 min, 30 min, 1 h, 2 h, 4 h, 6 h, 8 h, 12 h, 24 h, 48 h and 72 h after the injection with an IVIS imaging system (Perkin Elmer, USA). Dye accumulation and retention in tumors was evaluated quantitatively by calculating the ROI values.

The tumor-bearing mice were killed at 2 h, 8 h, 24 h, 48 h and 72 h after the polymer micelles were injected, and then the livers, hearts, spleens, lungs, kidneys and tumors were collected for isolated organ imaging to estimate the tissue

distribution of the micelles. We evaluated the fluorescence intensity of tissues quantitatively by calculating the ROI values.

Tissue slices

The livers, hearts, spleens, lungs, kidneys and tumors tissues were used to make tissue slices which were harvested at 2 h, 8 h, 24 h, 48 h and 72 h after the MPEG-PDLLA micelles were injected [58]. In detail, an embedding medium was used to fix the tissues and get tissue slices using a frozen section machine. Then DAPI was added for 5 min and they were sealed with glycerine. A confocal laser scanning microscope (CLSM) from Germany Leica Corporation was used to observe the fluorescence intensity of the tissues.

Statistics

Statistical analysis was performed using a Student's t-test or one-way analysis of variance (ANOVA). All data were expressed as the mean value ± SD. *P* values less than 0.05 were considered to be statistically significant.

Results and discussion

Characterization of MPEG-PDLLA-NH_2

In this study, we successfully synthesized the MPEG-PDLLA-NH_2 block copolymer and reacted it with the fluorescence marker cy5.5 dye. The synthesis route is illustrated in Fig. 1. In detail, the MPEG-PDLLA copolymer was synthesized by ring opening polymerization, then the BOC-L-AlA was converted into MPEG-PDLLA. Our target product was obtained by removing the tert-butoxycarbonyl end group from MPEG-PDLLA-BOC. MPEG-PDLLA, MPEG-PDLLA-BOC and MPEG -PDLLA-NH_2 were characterized by a ^{1}H NMR spectrum, and the molecular weights and polydispersity of the copolymer were determined by GPC. The molecular weight data of MPEG-PDLLA, MPEG-PDLLA-BOC and MPEG-PDLLA-NH_2 are summarized in Table. 1.

From the results of the ^{1}H NMR spectrum in Fig. 2, we can see four peaks marked with letters from a to d in Fig. 2 (A) MPEG-PDLLA, a at 3.62 ppm (CH_3O-), b at 3.63 ppm (-CH_2CH_2O-), c at 5.15 ppm (-$COCH(CH_3)O$-), d at 1.55 ppm (-CH_3). In the ^{1}H

NMR spectrum in Fig. 2 (B), the peak marked with letter e (1.39 ppm) represented the tert-butoxycarbonyl group, demonstrating that the BOC-terminated MPEG-PDLLA block polymer was successfully synthesized. The peak e (1.39 ppm) disappeared completely in Fig. 2 (C), since we eliminated the tert-butoxycarbonyl group and got MPEG-PDLLA-NH_2.

Analysis by GPC revealed the retention time of MPEG-PDLLA, MPEG-PDLLA-BOC and MPEG-PDLLA-NH_2 in Fig. 3. Fig. 3 (A) MPEG-PDLLA demonstrated a single peak with polydispersity of 1.24 and Mn of 3360. Fig. 3 (B) showed a shift to a later retention time for MPEG-PDLLA-BOC, which is consistent with an increase in Mn of 4147. Fig. 3 (C) MPEG-PDLLA-NH_2 revealed an almost similar shape and the same position of the retention time as Fig. 3 (B), indicating that the polymeric structure was kept unchanged and the molecular weight and distribution changed very little.

The IR spectra of MPEG-PDLLA, MPEG-PDLLA-BOC and MPEG-PDLLA-NH_2 are showed in Fig. 4. From Fig. 4 (A), the absorption peak at 1188.76 cm^{-1} and 1455.00 cm^{-1} can be seen to belong to the MPEG block. The peak at 1755.10 cm^{-1} was characteristic of the PDLLA block. The absorption peaks at 1526.61 cm^{-1} and 3324.82 cm^{-1} were attributed to the νNH stretch vibration in Fig. 4 (B), indicating that the tert-butoxycarbonyl group was added into MPEG-PDLLA block polymer successfully. νNH stretch vibration was also found at 3327.90 cm^{-1} and 1535.68 cm^{-1} in Fig. 4 (C).

Characterization of the MPEG-PDLLA micelles

In this study, we used two methods to prepare the MPEG-PDLLA polymer micelles with different particle sizes. The schematic illustration of the preparation of the MPEG-PDLLA polymer micelles and flow diagram of the experiment is shown in Fig. 5.

We used a thin-film hydration method to prepare MPEG-PDLLA micelles. During the procedure, the MPEG-PDLLA copolymer was distributed as a homogenous, amorphous thin-film. Then the copolymer self-assembled to a core-shell structure in the water system. The polymer micelles were obtained after filtering with a syringe filter (pore size: 220 nm). As shown in Fig. 6 (A), the particle size of the

MPEG-PDLLA polymer micelles measured by dynamic light scattering (DLS) was 24.59 ± 1.16 nm. In the morphology study, the same diameter of the MPEG-PDLLA polymer micelles was observed in the TEM image.

According to Fig. 6 (B), the particle size of MPEG-PDLLA polymer micelles prepared by ethanol injection method was 150.27 ± 1.62 nm. The TEM image showed the same diameter of the MPEG-PDLLA micelles.

The stability of the MPEG-PDLLA micelles with Cy5.5 fluorescence marker

To investigate the stability of the MPEG-PDLLA polymer micelles *in vitro* by this system, we used a fluorescence spectrophotometer to observe the fluorescence intensity of the polymer micelles at 5 min, 30 min, 1 h, 2 h, 4 h, 6 h, 8 h, 12 h, 24 h, 48 h and 72 h after the polymer micelles were prepared in Fig. 7. From the results, the fluorescence intensity of free cy5.5 dye, polymer micelles A (particle size 25 nm) and polymer micelles B (particle size 150 nm) followed the same trend and didn't decrease. It demonstrated that the fluorescence wasn't quenched until 72h. The fluorescence intensity of free Cy5.5 dye was lower than the polymer micelles A (particle size 25 nm) and the polymer micelles B (particle size 150 nm), indicating that the free Cy5.5 dye had been successfully loaded into the polymer micelles.

Cellular imaging

We investigated the cellular uptake efficiency of the MPEG-PDLLA polymer micelles over time qualitatively by using a confocal laser scanning microscope (CLSM). Here we compared the cellular uptake efficiency between the polymer micelles A (particle size 25 nm) and the polymer micelles B (particle size 150 nm) at 30 min, 1 h, 2 h, 4 h, 6 h after adding the polymer micelles. The result showed that the micelles A (particle size 25 nm) could more efficiently penetrate into the MCF-7 cells and the cellular uptake efficiency was time-dependent. This result consisted with the previous studies [17-20] as the cellular uptake of nano carriers are regulated by membrane tension, the optimal radius for endocytosis is on the order of 25-50 nm.

Fig. 8 (A) shows the pictures of MCF-7 cells incubated with the polymer micelles A (particle size 25 nm). After 0.5 hrs' incubation with the polymer micelles A (particle size 25 nm), the column of Cy5.5 was almost black. It could be seen that DAPI

stained nuclei were circumvented by the MPEG-PDLLA polymer micelles A at 1h, indicating that the polymer micelles A (particle size 25 nm) had been internalized into the cytoplasm of MCF-7 cells. Also the fluorescence intensity increased with the time.

From Fig. 8 (B), we can also see the polymer micelles B (particle size 150 nm) were internalized into the cytoplasm of MCF-7 cells and the fluorescence intensity increased with the time. It was noted that the red fluorescence intensity in Fig. 8 (A) was higher than that in Fig. 8 (B), demonstrating that cellular uptake was easier for the polymer micelles with smaller particle size.

Cellular uptake of the MPEG-PDLLA polymer micelles with different particle sizes at different times was studied quantitatively by measuring the percentage of internalized Cy5.5 in MCF-7 cells in Fig. 8 (C). After 0.5 hrs' incubation with the polymer micelles, 20.26 ± 2.81 % of the polymer micelles A (particle size 25 nm) and 18.37 ± 1.02 % of the polymer micelles B (particle size 150 nm) were internalized into the MCF-7 cells. After 6hrs' incubation, 56.02 ± 2.48 % of the polymer micelles A (particle size 25 nm) and 48.43 ± 2.08 % of the polymer micelles B (particle size 150 nm) were internalized into the MCF-7 cells respectively. The results indicated that between 30min and 6h, the polymer micelles showed time-dependent cellular uptake and the cellular uptake efficiency of the polymer micelles A (particle size 25 nm) was higher than the polymer micelles B (particle size 150 nm), demonstrating the same results as Fig. 8 (A) and Fig. 8 (B).

***In vivo* fluorescence imaging**

In vivo real-time biodistribution and tumor-target of the MPEG-PDLLA polymer micelles in MCF-7 tumor-bearing mice were evaluated through NIR florescence imaging with an IVIS imaging system at 5 min, 30 min, 1 h, 2 h, 4 h, 6 h, 8 h, 12 h, 24 h, 48 h and 72 h after being injected intravenously with the polymer micelles. The diagnosis profiles of polymer micelles A (particle size 25 nm), polymer micelles B (particle size 150 nm) and free Cy5.5 dye were clearly visualized by monitoring real-time NIR fluorescence intensity in the whole body as shown in Fig. 9.

According to Fig. 9 (A), the polymer micelles A (particle size 25 nm) had a time dependent biodistribution and tumor accumulation in mice bearing MCF-7 tumors.

Between 5 min and 72 h post-injection, the NIR fluorescence of the polymer micelles A (particle size 25 nm) increased fluorescence signals within the tumors, although decreased in the whole body, which may be due to specific targeting of tumor cells. We quantified the fluorescence intensity in the tumor by the ROI value in Fig. 9 (D). The ROI value showed that the fluorescence intensity at the tumor site didn't decrease until 72 h.

From the results in Fig. 9 (B), the administration of the polymer micelles B (particle size 150 nm) resulted in a fluorescence signal which gradually decreased with time. Between 5 min and 24 h after injection, the difference in the fluorescence intensity at the tumor site was smaller for MCF-7 tumor-bearing mice injected with either the polymer micelles A (particle size 25 nm) or the polymer micelles B (particle size 150 nm). However, at 48 h post-injection, the polymer micelles A (particle size 25 nm) showed a stronger fluorescence intensity at the tumor site than the polymer micelles B (particle size 150 nm). The same results are shown in Fig. 9 (D), demonstrating that the enhanced permeation and retention (EPR) effect was affected by particle size.

In this study, we used the group of free Cy5.5 dye as control group. From Fig. 9 (C), the fluorescence signal at the tumor was weaker than the whole body all the time. The quantitative fluorescence intensity measured by the ROI value in Fig. 9 (D) showed the same results, indicating that the tumor accumulation of fluorescence were due to the polymer micelles.

***In vitro* fluorescence imaging**

In this part, the MCF-7 tumor-bearing mice were killed at 2 h, 8 h, 24 h, 48 h and 72 h after the MPEG-PDLLA polymer micelles was injected intravenously, and then the livers, hearts, spleens, lungs, kidneys and tumors were isolated to estimate the tissue distribution of the polymer micelles using NIR florescence imaging with an IVIS imaging system.

The fluorescent signals of the MPEG-PDLLA polymer micelles in the deep organs were often underestimated in *in vivo* fluorescence imaging because of optical impedance by soft tissues. So the *in vitro* fluorescence imaging experiment shown in

Fig. 10 was necessary for us to study the tissue distribution of the polymer micelles.

From the results of the tissue distribution of the polymer micelles A (particle size 25 nm) in Fig. 10 (A), a significant enhancement of fluorescence signals was exhibited in tumors as the time extended, whereas the fluorescence intensity of the hearts, lungs, spleens decreased as the time extended. It was noted that the fluorescence intensity of the hearts showed only background to moderate signals, the acute cardiotoxicity of heart may have decreased. The fluorescence intensity of the livers and kidneys from mice treated with polymer micelles A (particle size 25 nm) also displayed strong signals and peaked at 8h post-injection, indicating that polymer micelles A (particle size 25 nm) were undergoing liver metabolism and renal excretion. In short, between 8 h and 72 h post-injection, the fluorescence intensity of other tissues gradually decreased with time, but the fluorescence intensity at the tumor site remained at a relatively high level indicating that the polymer micelles A had a long circulation time and the enhanced permeability and retention (EPR) effect of the tumor. The quantitative fluorescence intensity of the tissues measured by the ROI value in Fig. 10 (D) showed the same results.

According to Fig. 10 (B), the tissues showed almost the same results as the polymer micelles A (particle size 25 nm) except the tumors. The fluorescence intensity of the tumors showed a rise first, followed by a decline. The tumor tissues had the strongest fluorescence intensity at 8h post-injection and then decreased rapidly, demonstrating enhanced permeation and retention (EPR) effect was affected by particle size. The quantitative results measured by the ROI value showed in Fig. 10 (E) consisted with Fig. 10 (B).

In this study, we used the group of free Cy5.5 dye as a control group. From Fig. 10 (C) and Fig. 10 (F), the fluorescence signal of all tissues was weaker than the polymer micelle groups, indicating that the fluorescence of the tissue distribution was due to the polymer micelles.

Tissue slices

The distribution of MPEG-PDLLA polymer micelles was ever changing with time after injection. In this part, we observed the fluorescence intensity by a confocal laser

scanning microscope (CLSM) from the German Leica Corporation. The results of the images were shown in Fig. 11.

From the results of the tissue slice distribution of the polymer micelles A (particle size 25 nm) in Fig. 11 (A), the fluorescence intensity of the tumor tissue slices rose with the time and maintained the fluorescence signal until 72h post-injection. The fluorescence distribution in the livers and kidneys increased generally, and then decreased with time. The fluorescence signal of other tissue slices also decreased as the results showed in *in vitro* tissues fluorescence imaging.

Fig. 11 (B) showed the tissue slice distribution of the polymer micelles B (particle size 150 nm). Seen from imaging, we found that the fluorescence intensity of the livers and kidneys were a bit stronger than the micelles A (particle size 25 nm), but the tumor tissue had the strongest fluorescence intensity at 8h post-injection and then decreased rapidly, indicating that the particle size affected the permeation and retention (EPR) effect.

The results of the free Cy5.5 dye tissue slices were shown in Fig. 11 (C). The fluorescence intensity of the tissue slices were weaker than the group of the micelles A (particle size 25 nm) and the polymer micelles B (particle size 150 nm). These tissue slice results were same with the results of *in vivo* and *in vitro* fluorescence imaging.

Conclusion

In this study, we successfully synthesized the diblock polymer MPEG-PDLLA-NH_2 and characterized it by ^1H NMR spectra, FTIR and GPC. We used hydrophobic Cy5.5 free dye reacting with the MPEG-PDLLA-NH_2 to get the fluorescence marker MPEG-PDLLA-Cy5.5. Then we separately used a thin-film hydration method and ethanol injection method to get two different particle sizes polymer micelles. One was MPEG-PDLLA polymer micelles A (particle size 25 nm), the other was MPEG-PDLLA polymer micelles B (particle size 150 nm). The polymer micelles were characterized by DLS and TEM and a fluorescence spectrophotometer. In addition, the cellular uptake experiment on MCF-7 cells *in vivo* suggested the cellular

uptake was affected by particle size and time. Between 30 min and 6 h, the fluorescence intensity increased with the time, and the fluorescence intensity of small particle size was stronger than the large one. Furthermore, we detected biodistribution and tumor-target of MPEG-PDLLA polymer micelles in MCF-7 tumor-bearing mice by *in vivo* and *in vitro* fluorescence imaging and tissue slices. The results showed that the fluorescence intensity of free Cy5.5 dye was weaker than the group of the MPEG-PDLLA-Cy5.5 polymer micelles. It was noted that the fluorescence signal of tumor tissue which injected the polymer micelles A (particle size 25 nm) was stronger than the group of the polymer micelles B (particle size 150 nm), demonstrating that the polymer micelles A (particle size 25 nm) accumulated more easily at the tumor site than the polymer micelles B (particle size 150 nm). Therefore, MPEG-PDLLA polymer micelles based on two different particle sizes demonstrated that small particle sizes (25 nm) could have high cellular uptake efficiency and enhance the EPR effect in tumor tissue. In short, drug delivery systems with small particle sizes may have potential applications to deliver antitumor drugs. In the future, our research will focus on the relationship between the particle size and cellular uptake efficiency, tumor-target ability.

Acknowledgement

This work was financially supported by The National Science Fund for Distinguished Young Scholars (NSFC31525009), and Distinguished Young Scholars of Sichuan University (2011SCU04B18).

Competing Interests

The authors have declared that no competing interest exists.

References

[1] N. L. Anatoly and P. T. Vladimir, Adv. Drug Delivery Rev., 2004, 56, 1273.

[2] G. Thirumala, S. Snjezana, C. G. Martin, I. Lisbeth and S. D. Stanley, J Control Release., 1999, 57, 171.

[3] E. Praveen, M. Cyrus and B. Helen, J. Pharm. Sci., 2009, 98, 945.

[4] G. Srinivas and A. Mansoor, Mol Pharm., 2009, 6, 928.

[5] Q. Chen, X. Wang, C. Wang, L. Z. Feng, Y. G. Li and Z. Liu, ACS Nano, 2015, 5, 5223.

[6] K. Y. Huang, H. L. Ma, J. Liu, S. D. Huo, K. Anil, T. Wei, X. Zhang, S. B. Jin, Y. L. Gan, P. C. Wang, S. T. He, X. N. Zhang and X. J. Liang, ACS Nano, 2012, 6, 4483.

[7] J. R. Peng, T. T. Qi, J. F. Liao, M. Fan, F. Luo, H. Li and Z. Y. Qian, Nanoscale, 2012, 4, 2694.

[8] W. N. Joseph and H. B. You, J Control Release., 2014, 190, 451.

[9] M. H. Tan, J. Luo and Y. Tian, RSC Adv., 2014, 4, 61948.

[10] L. Dai, C. X. Li, K. F. Liu, H. J. Su, B. Q. Chen, G. F. Zhang, J. He and J. D Lei, RSC Adv., 2015, 5, 15612.

[11] S. Liang, X. Jin, Y. F. Ma, J. Guo and H. Wang, RSC Adv., 2015, 5, 88560.

[12] D. Peer, J. M. Karp, S. Hong, O. C. Farokhzad, R. Margalit and R. Langer, Nature Nanotech., 2007, 2, 751.

[13] J. W. Kim, Y. M. Lee, Y. N. Kang and W. J. Kim, ACS Nano, 2014, 8, 9358.

[14] F. Lu, S. H. Wu, Y. Hung and C. Y. Mou, Small, 2009, 5, 1408.

[15] H. Cabral, Y. Matsumoto, K. Mizuno, Q. Chen, M. Murakami, M. Kimura, Y. Terada, M. R. Kano, K. Miyazono, M. Uesaka, N. Nishiyama and K. Kataoka, Nature Nanotech., 2011, 6, 815.

[16] P. Kyoungweon, K. Hilmar and R. A.Vaia, Nano Lett., 2010, 10, 1433.

[17] S. L. Zhang, J. Li, G. Lykotrafitis, G. Bao and S. Suresh, Adv. Mater., 2009, 21, 419.

[18] A. E. Nel, L. Mädler, D. Velegol, T. Xia, E. M. V. Hoek, P. somasundaran, F. Klaessiget, V. Castranova and M. Thompson, Nature materials, 2009, 8, 543.

[19] W. Zauner, N. A. Farrow and A. M. R. Haines, J Control Release., 2001, 71, 39.

[20] E. Oh, J. B. Delehanty, K. E. Sapsford, K. Susumuet, R. Goswami, J. B. B. Canosa, P. E. Dawson, J. Granek, M. Shoff, Q. Zhang, P. L. Goering, A. Huston and I. L. Medintz, ACS nano, 2011, 5, 6434.

[21] F. F An, Y. L. Yang, J. Liu, J. Ye, J. F. Zhang, M. J. Zhou, X. J. Zhang, C. J. Zheng, X. J. Liang and X. H. Zhang, RSC Adv., 2014, 4, 6120.

[22] F. Bensaid, O. T. D. Boullay, A. Amgoune, C. Pradel, L. H. Reddy, E. Didier, S. Sablé, G. Louit, D. Bazile and D. Bourissou, Biomacromolecules, 2013, 14, 1189.

[23] Y. H. Wen, R. G. Monica, L. F. Nielsen, L. Jorgensen, E. H. Møller and H. M. Nielsen, Eur J Pharm and Biopharm., 2013, 85, 87.

[24] C. Wang, Y. J. Wang, Y. J. Wang, M. Fan, F. Luo and Z. Y. Qian, Int J Pharm., 2011, 414, 251.

[25] F. Cui, Y. Li, S. F. Zhou, M. M. Jia, X. R. Yang, F. Yu, S. F. Ye, Z. Q. Hou and L. Y. Xie, Nanoscale Res Lett., 2013, 8, 301.

[26] F. M. Veronese and G. Pasut, Drug Discov Today., 2005, 10, 1451.

[27] S. S. Feng, Expert Rev. Medical Devices., 2004, 1, 115.

[28] S. W. Lee, M. H. Yun, S. W. Jeong, C. H. In, J. Y. Kim, M. H. Seo, C. M. Pai and S. O. Kim, J Control Release., 2011, 155, 262.

[29] X. L. Zheng, B. Kan, M. L. Gou, S. Z. Fu, J. Zhang, K. Men, L. J. Chen, F. Luo, Y. L. Zhao, X. Zhao, Y. Q. Wei and Z. Y. Qian, Int J Pharm., 2010, 386.

[31] X. X. Jin, Y. L. Wang, L. W. Tan, Y. He, J. R. Peng, L. Hai, Y. Wu and Z. Y. Qian, Nanomedicine, 2015, 10, 2153.

[32] Q. Zhao, Y. Hao, P. Y. Xu, J. Li, X. N. Zhang and Z. Y. Qian, Int J Nanomed., Under review.

[33] S. D. Huo, H. L. Ma, K. Y. Huang, J. Liu, T. Wei, S. B. Jin, J. C. Zhang, S. T. He and X. J. Liang, Cancer Res., 2013, 73, 319.

[34] M. H. Amtenbrink, D. W. Grainger and H. Hofmann, Nanomedicine: Nanotechnology, Biology, and Medicine, 2015, 11, 1689.

[35] R. A. Petros and J. M. DeSimone, Nature Reviews Drug Discovery, 2010, 9, 615.

[36] K. Chen, L. P. Yap, R. Y. Park, X. L. Hui, K. C. Wu, D. M. Fan, X. Y. Chen and P.

S. Conti, Amino Acids, 2012, 42, 1329.

[37] Z. Cheng, L. Jelena, Z. M. Xiong, O. Gheysens, S. Keren, X. Y. Chen, and S. S. Gambhir, Bioconjugate Chem., 2006, 17, 662.

[38] M. F. Kircher, U. Mahmood and R. S. King, Cancer Res., 2003, 63, 8122.

[39] R. Namgun, Y. M. Lee, J. Kim, Y. Jang, B. H. Lee, I. S. Kim, P. Sokkar, Y. M. Rhee, A. S. Hoffman and W. J. Kim, Nat. Commun., 2014, 5, 3702.

[40] M. Veiseh, P. Gabikian and S. B. Bahrami, Cancer Res., 2007, 67, 6882.

[41] L. Zhu, J. Xie, M. Swierczewska, F. Zhang, Q. M. Quan, Y. Ma, X. X. Fang, K. Kim, S. Lee and X. Y. Chen, Theranostics, 2011, 1, 18.

[42] G. Q. Li, Y. Xing, J. Wang, P. S. Conti and K. Chen, Amino Acids, 2014, 46, 1547.

[43] Y. C. Dong and S. S. Feng, Biomaterials, 2004, 25, 2843.

[44] C. Deng, G. Z. Rong, H. Y. Tian, Z. H. Tang, X. S. Chen and X. B. Jing, Polymer, 2005, 46, 653.

[45] P. F. Liu, H. Yu, Y. Sun, M. J. Zhu and Y. R. Duan, Biomaterials, 2012, 33, 4403.

[46] C. Deng, H. Y. Tian, P. B. Zhang, J. Sun, X. S. Chen and X. B. Jing, Biomacromolecules, 2006. 7. 590.

[47] Z. B. Li, Q. L. Jin, C. W. Huang, S. Dasa, L. H. Chen, L. P. Yap, S. L. Liu, H. C. Cai, R. Park and P. S. Conti, Theranostics, 2011, 1, 371.

[48] S. Y. Lee, M. S. Huh, S. K. Lee, S. J. Lee, H. J. Chung, J. H. Park, Y. K Oh, K. Choi, K. Kim and I. C. Kwon, J Control Release., 2010, 141, 339.

[49] Y. J. Wang, L. J. Chen, L. W. Tan, Q. Zhao, F. Luo, Y. Q. Wei and Z. Y. Qian, Biomaterials, 2014, 35, 6972.

[50] L. Q. Zou, W. Liu, W. L. Liu, R. H. Liang, T. Li, C. M. Liu, Y. L. Cao, J. Niu and Z. Liu, J. Agric. Food Chem., 2014; 62, 934.

[51] Y. S. Maitani, H. S. Soeda, J. P. Wan and K. Takayama, J Liposome Res., 2001, 11, 115.

[52] J. F. Wang, W. M. Liu, Q. Tu, J. C. Wang, N. Song, Y. R. Zhang, N. Nie and J. Y. Wang, Biomacromolecules, 2011, 2, 228.

[53] J. E. Chung, S. Tan, S. J. Gao, N. Yongvongsoontorn, S. H. Kim, J. H. Lee, H. S.

Choi, H. Yano, L. Zhuo and M. Kurisawa, Nature Nanotech., 2014, 208, 1.

[54] H. Y. Nam, S. M. Kwon, H. Chung, S. H. Lee, S. H. Kwon, H. Jeon, Y. Kim, J. H. Park, J. Kim, S. Her, Y. K. Oh, I. C. Kwon, K. Kim and S. Y. Jeong, J Control Release., 2009, 135, 259.

[55] J. F. Stefanick, J. D. Ashley, T. Kiziltepe and B. Bilgicer, ACS Nano, 2013, 4, 2935.

[56] C. L. Peng, Y. H. Shih, P. C. Lee, T. M. H. Hsieh, T. Y. Luo and M. J. Shieh, ACS Nano, 2011, 7, 5594.

[57] J. F. Liao, W. T. Li, J. R. Peng, Q. Yang, H. Li, Y. Q. Wei, X. N. Zhang and Z. Y. Qian, Theranostics, 2015, 5, 345.

[58] Q. J. He, Z. W. Zhang, F. Gao, Y. P. Li and J. L. Shi, Small, 2011, 7, 271.

Figure Captions:

Fig. 1 The synthesis route of MPEG-PDLLA-Cy5.5.

Table. 1 The molecular weight data of MPEG-PDLLA, MPEG-PDLLA-BOC and MPEG-PDLLA-NH_2.

Fig. 2 The ^{1}HNMR spectra of (A) MPEG-PDLLA, (B) MPEG-PDLLA-BOC, (C) MPEG-PDLLA-NH_2 in $CDCl_3$.

Fig. 3 The retention time of (A) MPEG-PDLLA, (B) MPEG-PDLLA-BOC, (C) MPEG-PDLLA-NH_2 measured by GPC.

Fig. 4 The IR spectra of (A) MPEG-PDLLA, (B) MPEG-PDLLA-BOC, (C) MPEG-PDLLA-NH_2.

Fig. 5 The schematic illustration of the preparation of the MPEG-PDLLA polymer micelles and flow diagram of the experiment.

Fig. 6 The particle size distribution and TEM (inset image) of the MPEG-PDLLA polymer micelles, (A) MPEG-PDLLA polymer micelles (particle size 25 nm), (B) MPEG-PDLLA polymer micelles (particle size 150 nm).

Fig. 7 The fluorescence intensity of the polymer micelles A (particle size 25 nm), the polymer micelles B (particle size 150 nm) and free Cy5.5 Dye *in vitro* at 5 min, 30 min, 1 h, 2 h, 4 h, 6 h, 8 h, 12 h, 24 h, 48 h and 72 h. The data points represent mean values and the bars represent standard deviation. (n = 3).

Fig. 8 The cell uptake of (A) The polymer micelles A (particle size 25 nm),

(B) The polymer micelles B (particle size 150 nm) at 30 min, 1 h, 2 h, 4 h and 6 h. (Column 1: Cy5.5 channels showing red fluorescence from the MPEG-PDLLA polymer micelles distributed in the cytoplasm.

Column 2: DAPI channels showing blue fluorescence from nuclei.

Column 3: Merged channels of Cy5.5 and DAPI.)

(C) The quantitative data analyzed by flow cytometry. The data points represent mean values and the bars represent standard deviation. (n = 3). The double star (**) indicates $P< 0.01$.

Fig. 9 *In vivo* time-dependent fluorescence image in MCF-7 tumor-bearing mice at 5 min, 30 min, 1 h, 2 h, 4 h, 6 h, 8 h, 12 h, 24 h, 48 h and 72 h after being injected

intravenously with the polymer micelles. The color bar from red to blue indicates the change in fluorescence signal intensity from low to high.

(A)The polymer micelles A (particle size 25 nm),

(B) The polymer micelles B (particle size 150 nm),

(C) The free Cy5.5 dye,

(D) The quantitative fluorescence intensity measured by RIO value. The data points represent mean values and the bars represent standard deviation. (n = 3). The double star (**) indicates $P< 0.01$.

Fig. 10 *In vitro* imaging of the livers, hearts, spleens, lungs, kidneys and tumors excised from MCF-7 tumor-bearing mice at 2 h, 8 h, 24 h, 48 h and 72 h after being injected intravenously with the polymer micelles. The color bar from red to blue indicates the change in fluorescence signal intensity from low to high.

(A)The polymer micelles A (particle size 25 nm),

(B) The polymer micelles B (particle size 150 nm),

(C) The free Cy5.5 dye.

The quantitative fluorescence intensity of tissues measured by RIO value.

(D)The polymer micelles A (particle size 25 nm),

(E) The polymer micelles B (particle size 150 nm),

(F) The free Cy5.5 dye.

Fig. 11 Fluorescence images of the livers, hearts, spleens, lungs, kidneys and tumors tissue slices from MCF-7 tumor bearing mice at 2 h, 8 h, 24 h, 48 h and 72 h after being injected intravenously with the polymer micelles.

(A)The polymer micelles A (particle size 25 nm),

(B) The polymer micelles B (particle size 150 nm),

(C) The free Cy5.5 dye.

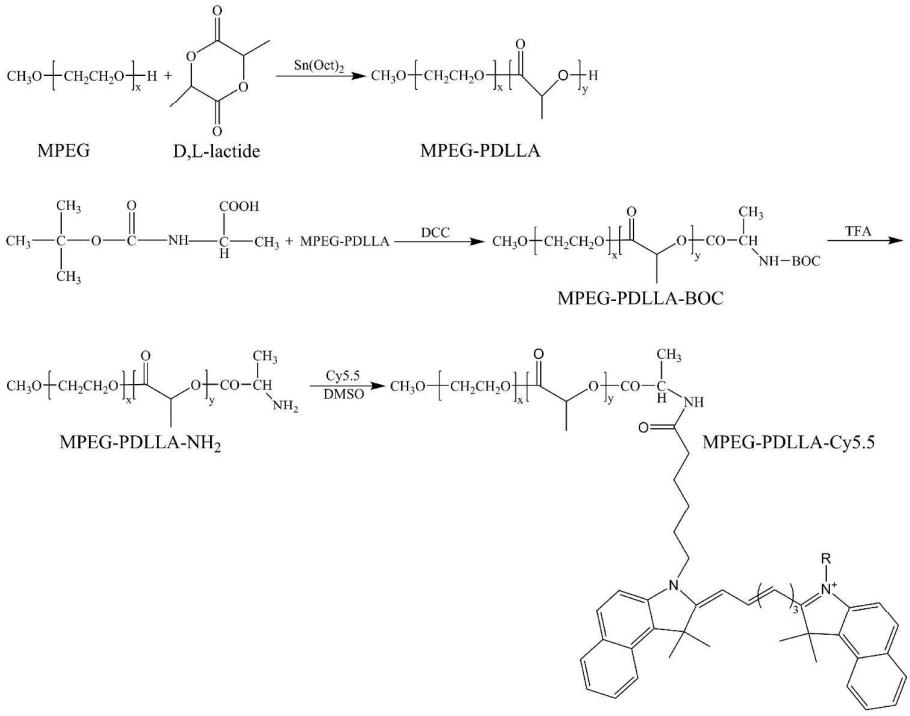

Fig. 1 The synthesis route of MPEG-PDLLA-Cy5.5.

603
604
605
606
607

608 **Table. 1** The molecular weight data of MPEG-PDLLA, MPEG-PDLLA-BOC and
609 MPEG-PDLLA-NH_2

Sample	Mn^1	Mn^2	Mn^3	Mw^3	Mw^3/Mn^3
MPEG-PDLLA	3765	3821	3360	4152	1.24
MPEG-PDLLA-BOC	3850	4315	4147	4649	1.12
MPEG-PDLLA-NH_2	3950	3980	4234	4902	1.16

610 [1] Theoretical molecular weight. [2] Calculated from ^{1}HNMR data. [3] measured by GPC.

611
612
613

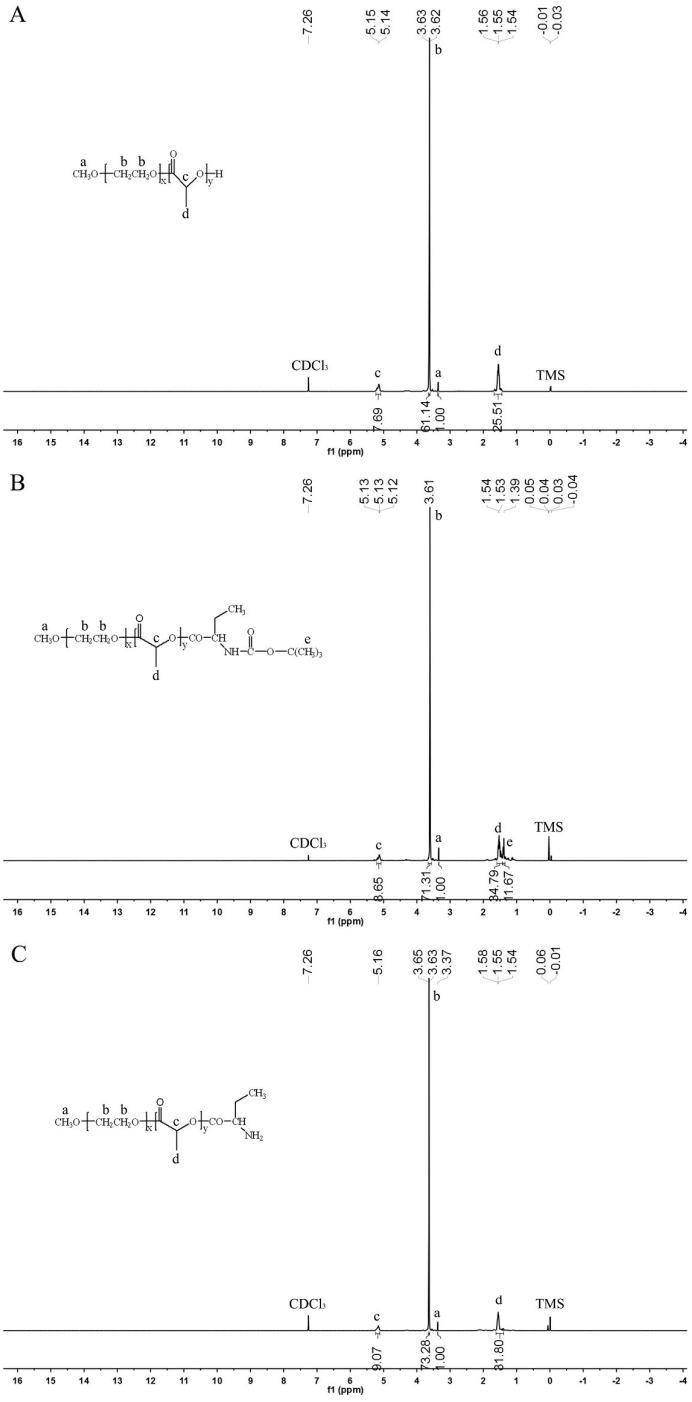

Fig. 2 The ^{1}HNMR spectra of (A) MPEG-PDLLA, (B) MPEG-PDLLA-BOC, (C) MPEG-PDLLA-NH_2 in $CDCl_3$.

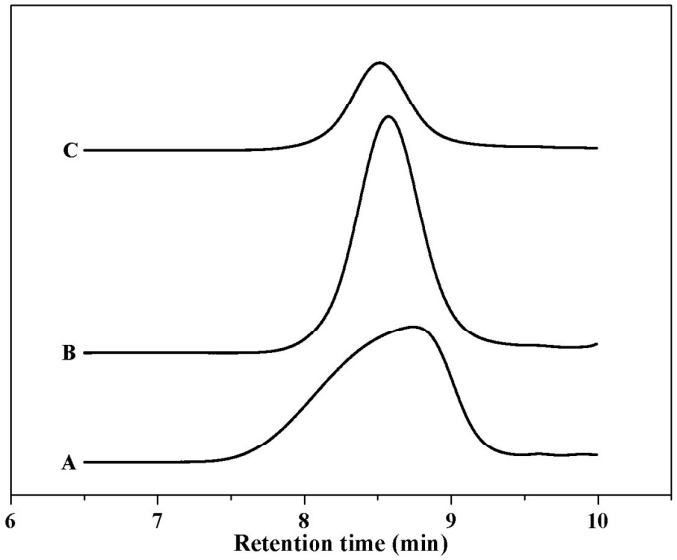

Fig. 3 The retention time of (A) MPEG-PDLLA, (B) MPEG-PDLLA-BOC, (C) MPEG-PDLLA-NH_2 measured by GPC.

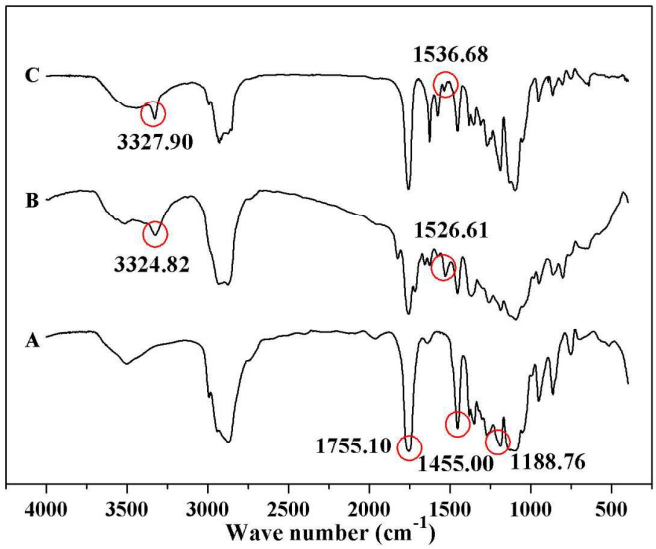

Fig. 4 The IR spectra of (A) MPEG-PDLLA, (B) MPEG-PDLLA-BOC, (C) MPEG-PDLLA-NH_2.

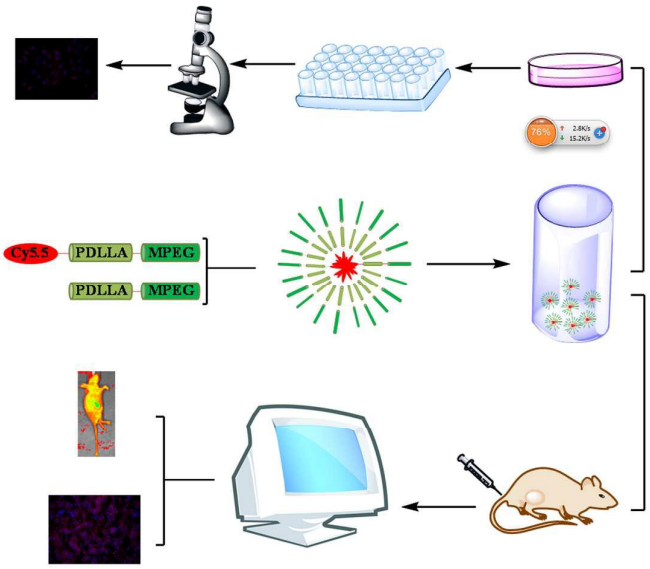

Fig. 5 The schematic illustration of the preparation of the MPEG-PDLLA polymer micelles and flow diagram of the experiment.

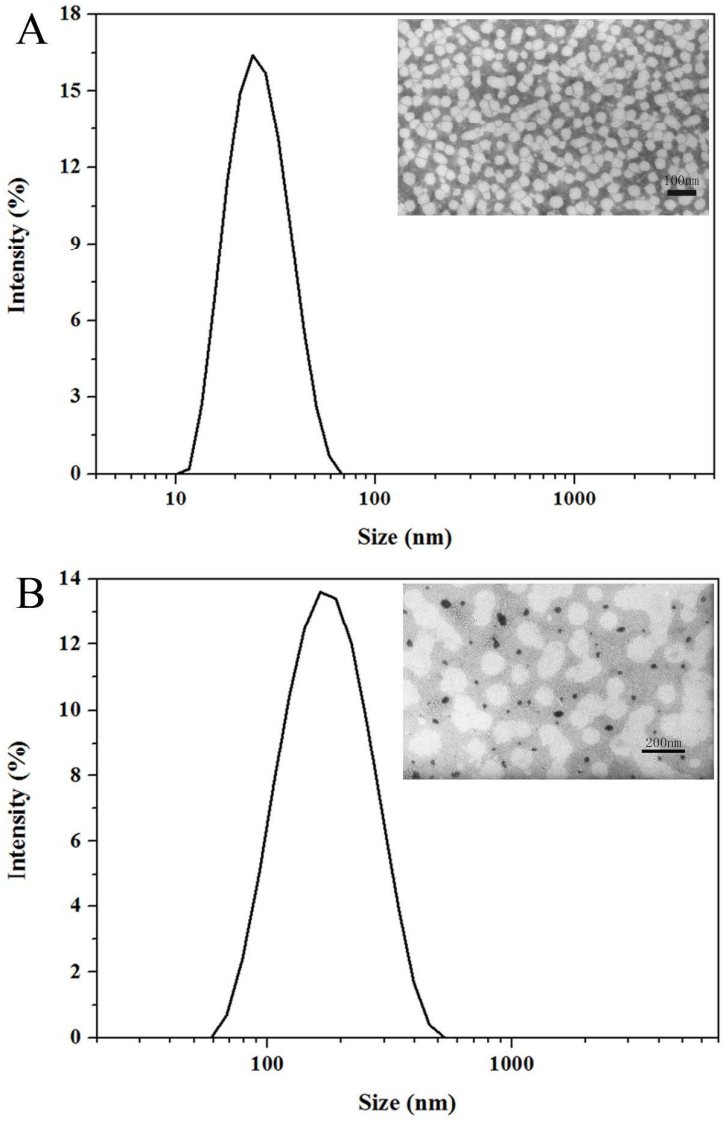

Fig. 6 The particle size distribution and TEM (inset image) of the MPEG-PDLLA polymer micelles, (A) MPEG-PDLLA polymer micelles (particle size 25 nm), (B) MPEG-PDLLA polymer micelles (particle size 150 nm).

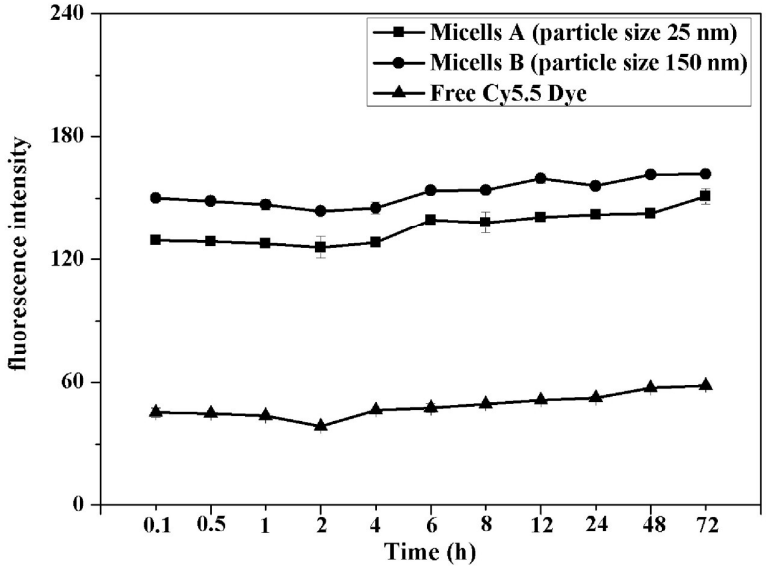

Fig. 7 The fluorescence intensity of the polymer micelles A (particle size 25 nm), the polymer micelles B (particle size 150 nm) and free Cy5.5 Dye *in vitro* at 5 min, 30 min, 1 h, 2 h, 4 h, 6 h, 8 h, 12 h, 24 h, 48 h and 72 h. The data points represent mean values and the bars represent standard deviation. (n = 3).

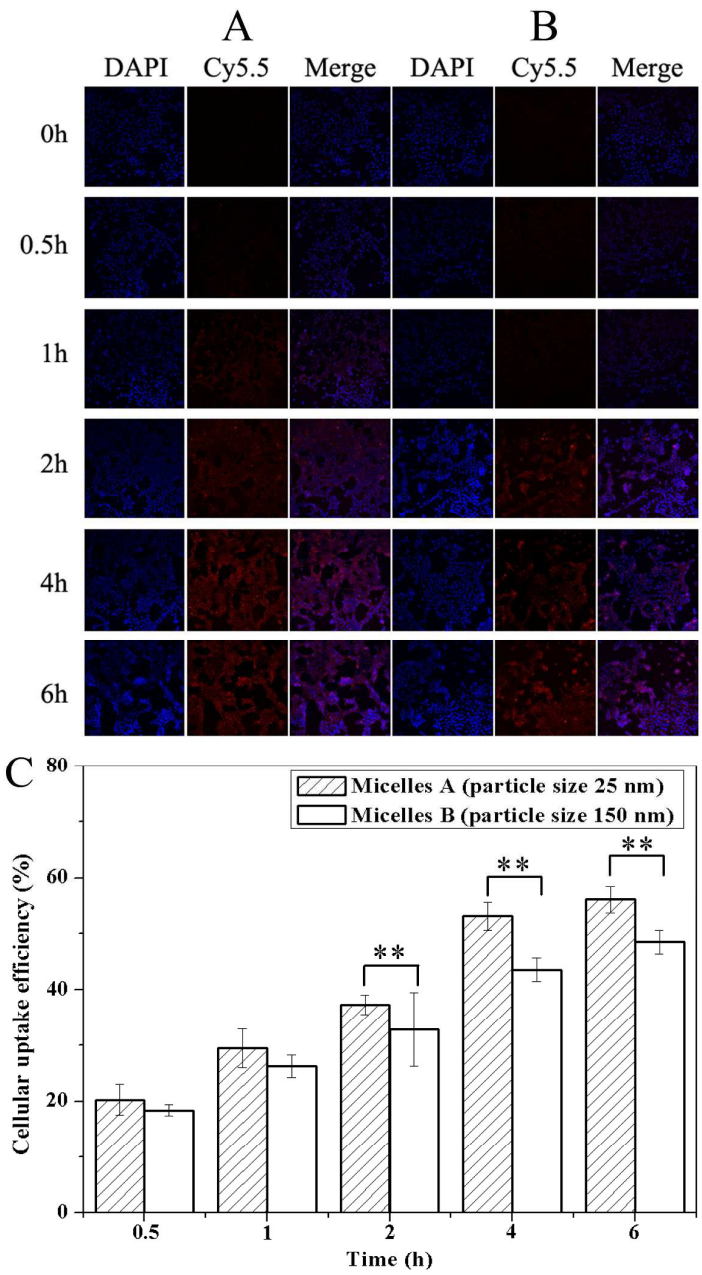

Fig. 8 The cell uptake of (A) The polymer micelles A (particle size 25 nm), (B) The polymer micelles B (particle size 150 nm) at 30 min, 1 h, 2 h, 4 h and 6 h. (Column 1: Cy5.5 channels showing red fluorescence from the MPEG-PDLLA polymer micelles distributed in the cytoplasm. Column 2: DAPI channels showing blue fluorescence from nuclei. Column 3: Merged channels of Cy5.5 and DAPI.) (C) The quantitative data analyzed by flow cytometry. The data points represent mean values and the bars represent standard deviation. (n = 3). The double star (**) indicates $P < 0.01$.

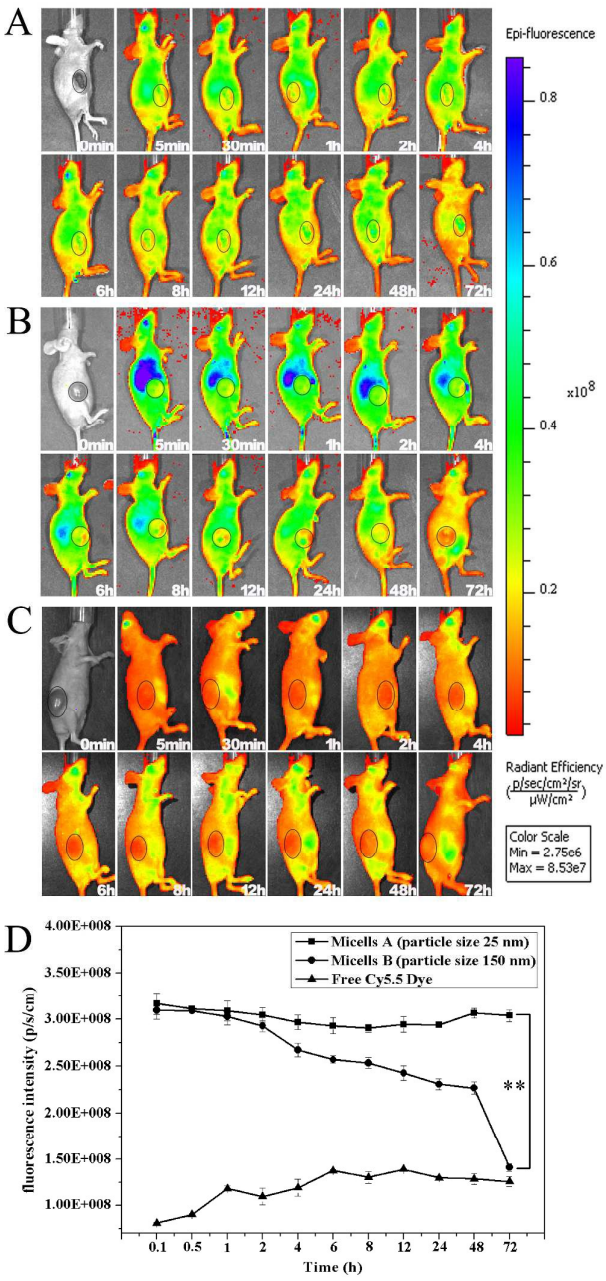

Fig. 9 *In vivo* time-dependent fluorescence image in MCF-7 tumor-bearing mice at 5 min, 30 min, 1 h, 2 h, 4 h, 6 h, 8 h, 12 h, 24 h, 48 h and 72 h after being injected intravenously with the polymer micelles. The color bar from red to blue indicates the change in fluorescence signal intensity from low to high. (A) The polymer micelles A (particle size 25 nm), (B) The polymer micelles B (particle size 150 nm), (C) The free Cy5.5 dye, (D) The quantitative fluorescence intensity measured by RIO value. The data points represent mean values and the bars represent standard deviation. (n = 3). The double star (**) indicates $P < 0.01$.

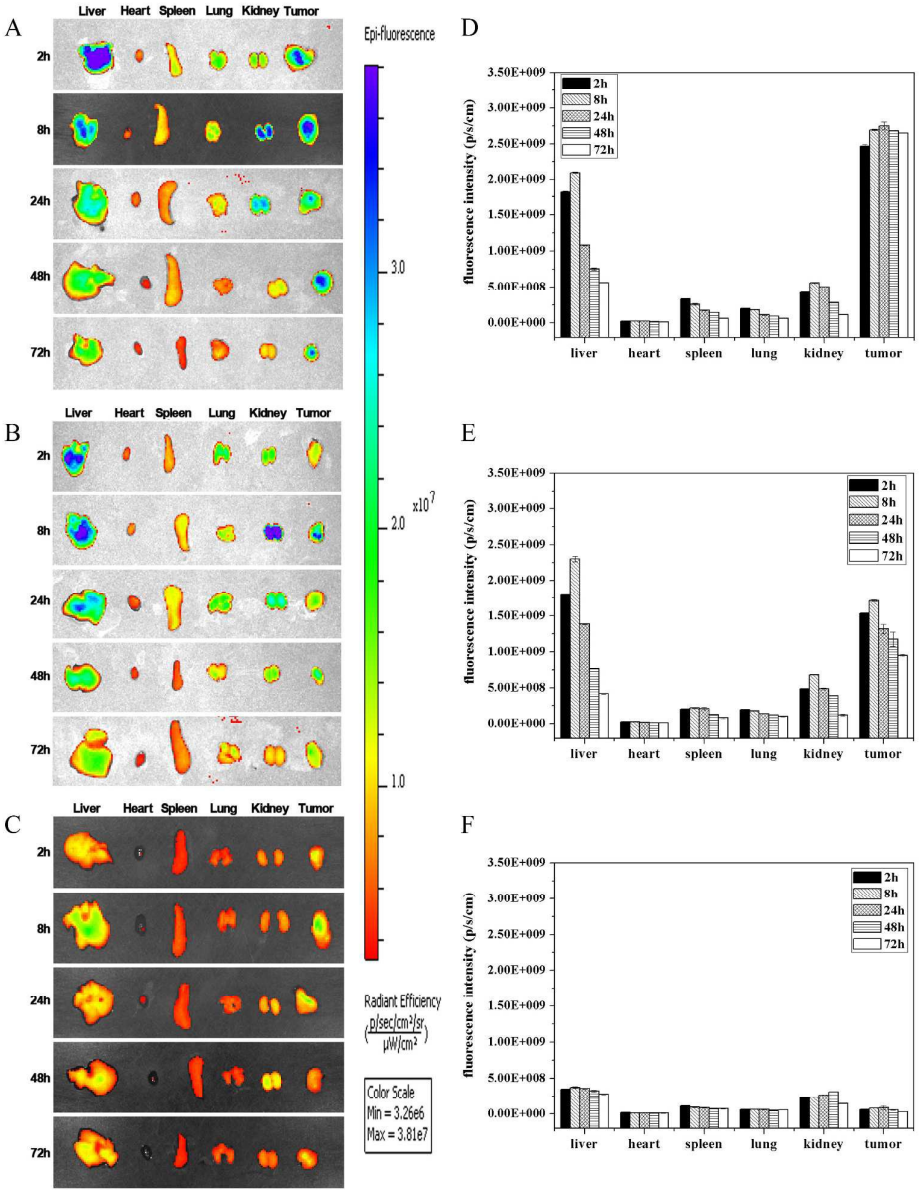

Fig. 10 *In vitro* imaging of the livers, hearts, spleens, lungs, kidneys and tumors excised from MCF-7 tumor-bearing mice at 2 h, 8 h, 24 h, 48 h and 72 h after being injected intravenously with the polymer micelles. The color bar from red to blue indicates the change in fluorescence signal intensity from low to high. (A) The polymer micelles A (particle size 25 nm), (B) The polymer micelles B (particle size 150 nm), (C) The free Cy5.5 dye. The quantitative fluorescence intensity of tissues measured by RIO value. (D) The polymer micelles A (particle size 25 nm), (E) The polymer micelles B (particle size 150 nm), (F) The free Cy5.5 dye.

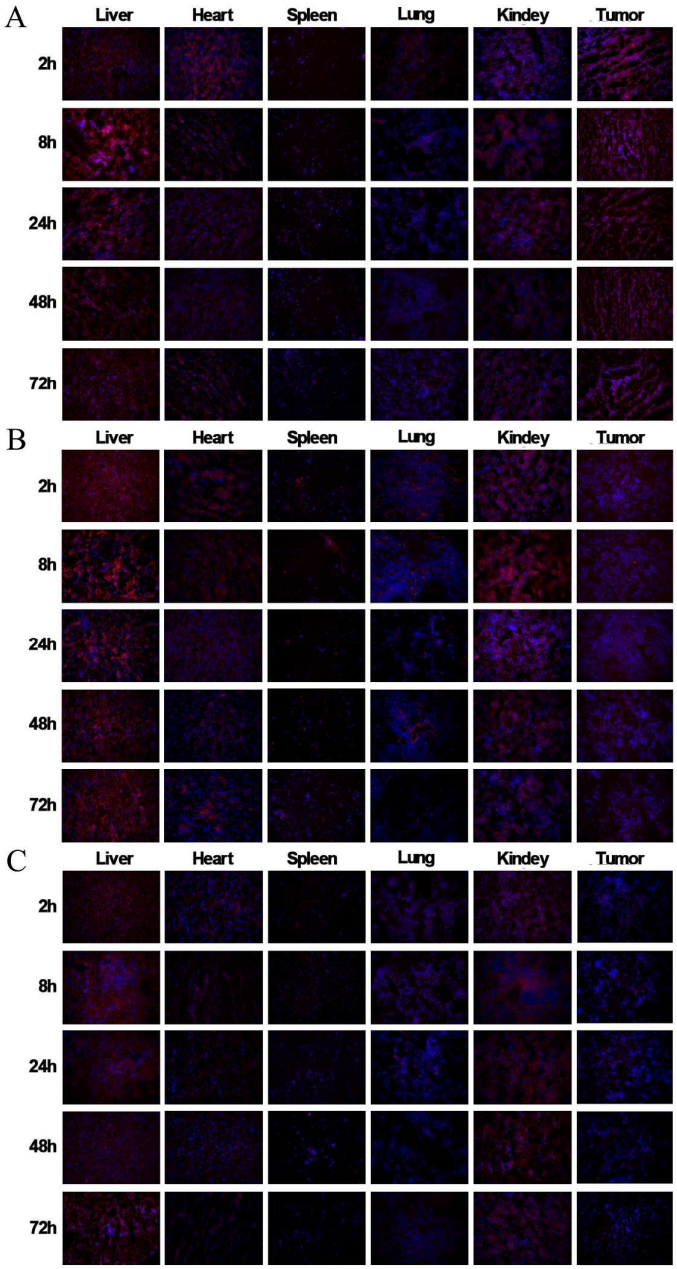

Fig. 11 Fluorescence images of the livers, hearts, spleens, lungs, kidneys and tumors tissue slices from MCF-7 tumor-bearing mice at 2 h, 8 h, 24 h, 48 h and 72 h after being injected intravenously with the polymer micelles. (A) The polymer micelles A (particle size 25 nm), (B) The polymer micelles B (particle size 150 nm), (C) The free Cy5.5 dye.

Contents entry graphic

The study reported herein describes the cellular uptake efficiency and tumor-target ability of MPEG-PDLLA micelles with two different particle sizes.